

# Single-Molecule Magnet Behavior and Magnetocaloric Effect in Ferromagnetically Coupled $\text{Ln}^{\text{II}}\text{-Ni}^{\text{II}}\text{-Ni}^{\text{II}}\text{-Ln}^{\text{III}}$ ( $\text{Ln}^{\text{III}} = \text{Dy}^{\text{III}}$ and $\text{Gd}^{\text{III}}$ ) Linear Complexes†

Carlos Meseguer,<sup>a</sup> Silvia Titos-Padilla,<sup>a</sup> Mikko M. Hänninen,<sup>b</sup> R. Navarrete,<sup>c</sup> A. J. Mota, Marco Evangelisti,<sup>d</sup> José Ruiz,<sup>a</sup> Enrique Colacio<sup>\*,a</sup>

<sup>a</sup>*Departamento de Química Inorgánica, Facultad de Ciencias, Universidad de Granada. Avda. Fuentenueva s/n, 18071-Granada, Spain.*

<sup>b</sup>*Department of Chemistry, University of Jyväskylä, P. O. Box 35, 40014 Jyväskylä, Finland.*

<sup>c</sup>*Departamento de Química Inorgánica, Facultad de Farmacia, Campus de Cartuja, 18071 Granada, Spain.*

<sup>d</sup>*Instituto de Ciencia de Materiales de Aragón (ICMA), CSIC-Universidad de Zaragoza, Departamento de Física de la Materia Condensada, 50009 Zaragoza, Spain.*

† *This paper is dedicated to the memory of one of the authors, our lovely friend José Ruiz, who just recently died.*

## Abstract

A new type of linear tetranuclear  $\text{Ln}^{\text{III}}\text{-Ni}^{\text{II}}\text{-Ni}^{\text{II}}\text{-Ln}^{\text{III}}$  ( $\text{Ln}^{\text{III}} = \text{Dy}$  **1**,  $\text{Gd}$  **2**) complexes have been prepared using multidentate ligand *N,N'*-bis(3-methoxysalicylidene)-1,3-diaminobenzene having two sets of NO and OO' coordination pockets which can selectively accommodate  $\text{Ni}^{\text{II}}$  and  $\text{Ln}^{\text{III}}$  ions, respectively. The X-ray structure analysis reveals that the  $\text{Ni}^{\text{II}}$  ions are bridged by phenylenediimine groups forming a twelve-membered metallacycle in the central body of the complex, whereas the  $\text{Ln}^{\text{III}}$  ions are located at both sides of the metallacycle and linked to the  $\text{Ni}^{\text{II}}$  ions by diphenoxo

bridging groups. Phenylenediimine and diphenoxo bridging groups transmit ferromagnetic exchange interactions between the two Ni<sup>II</sup> ions but also between Ni<sup>II</sup> and Ln<sup>III</sup> ions, respectively. Complex **1** shows slow relaxation of the magnetization at zero-field and a thermal energy barrier  $U_{\text{eff}} = 7.4$  K with  $H_{\text{dc}} = 1000$  Oe, whereas complex **2** exhibits an  $S = 9$  ground state and significant magnetocaloric effect ( $-\Delta S_{\text{m}} = 18.5$  J kg<sup>-1</sup> K<sup>-1</sup> at  $T = 3$  K and  $\Delta B = 5$  T).

## Introduction

In recent years the area of molecular magnetism based heterometallic 3d-4f complexes has undergone a renaissance with the finding that many of these systems can behave as Single-Molecule Magnets (SMMs)<sup>1</sup> or low temperature Molecular Magnetic Coolers (MMCs).<sup>2</sup> SMMs exhibit slow relaxation of the magnetization and magnetic hysteresis below a blocking temperature ( $T_{\text{B}}$ )<sup>3</sup> and have been proposed as potential candidates for applications in molecular spintronics, ultra-high density magnetic information storage and quantum computing at molecular level.<sup>4</sup> The SMM behavior is due to the existence of an energy barrier ( $U$ ) that prevents reversal of the magnetization when the magnetic field is brought to zero, leading to bistability of the ground state.<sup>3</sup> MMCs, in turn, show enhanced magneto-caloric effect (MCE), that is, the change of magnetic entropy ( $\Delta S_{\text{m}}$ ) and adiabatic temperature provoked by the change of an applied magnetic field, which can be potentially used for cryogenic applications.<sup>2,5</sup> Thus, these systems have been proposed as possible alternatives to very-low-temperature technologies and for cryogenic sensors in aerospace devices.<sup>2,5</sup>

Both SMMs and MMCs require large multiplicity in the ground state, which can be guaranteed in the 3d-4f systems by the presence of the lanthanide ion. However, the

anisotropy of the system plays completely different role in SMMs and MMCs. While MMCs should possess a ground state with negligible anisotropy, SMMs require a highly anisotropic ground state, as the height of the energy barrier for the relaxation of the magnetization depends on the anisotropy of the state. It should be noted that the 3d-4f magnetic exchange interactions are very weak, due to the very efficient shielding of the 4f orbitals of the Ln<sup>III</sup> ion by the fully occupied 5s and 5p orbitals, and, for the second half of the lanthanide series, generally ferromagnetic in nature.<sup>6</sup> Therefore, ground states with large spin multiplicity, as well as multiple low-lying excited and field-accessible states are generated, each of which can contribute to the magnetic entropy of the system enhancing the MCE effect. Moreover, it is worth mentioning that a large MCE can only be observed when the 3d-4f complex possesses a small molar mass with a large metal/ligand mass ratio, in order to limit the amount of passive, non-magnetic elements.<sup>4,7</sup> Taking into account the above considerations, small 3d-4f complexes, containing highly anisotropic Dy<sup>III</sup> ions could be, in principle, good candidates to show SMM behavior, while those bearing isotropic Gd<sup>III</sup> ions could exhibit large MCE and thus MMC behavior.<sup>4,7</sup> It is however worth pointing out that SMM and MMC behaviors are closely interrelated to each other, depending on experimental conditions considered, as particularly evident in the recently investigated GdW<sub>30</sub> molecule<sup>8</sup> and also illustrated in reference 9.

In recent years, an increasing number of Ni-Dy polynuclear complexes have been reported.<sup>6,10</sup> While only few of them exhibit SMMs behavior, the MMC properties of their Ni-Gd counterparts have been barely studied.<sup>11</sup> Along these lines, we have exploited novel ditopic ligand H<sub>2</sub>L (N,N'-bis(3-methoxysalicylidene)-1,3-diaminobenzene), containing two coordination “pockets” (Figure 1) having NO and

OO' donor sets with preference for transition metal and lanthanide ions, respectively, and applied this ancillary in the synthesis of the Ni<sub>2</sub>Ln<sub>2</sub> complexes.

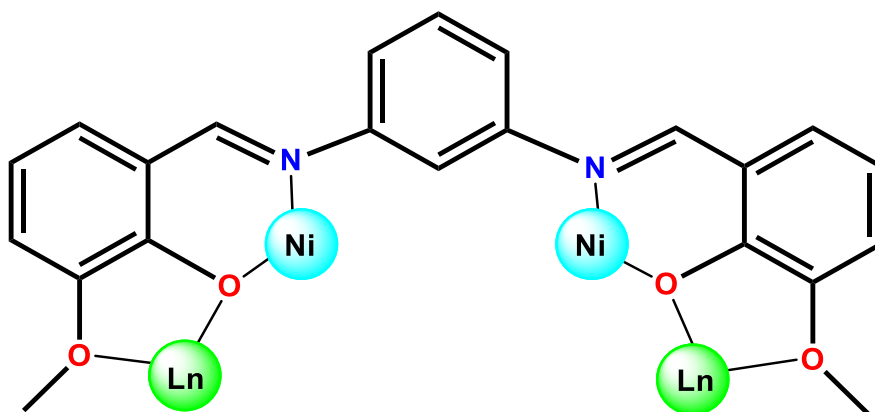


**Figure 1.**-Structure and coordination sites of the ligand H<sub>2</sub>L.

Herein, we report the synthesis, X-ray structure and detailed dc/ac magnetic studies of the complexes [LnNi(H<sub>2</sub>O)(CH<sub>3</sub>CN)(NO<sub>3</sub>)<sub>3</sub>(L)NiLn(H<sub>2</sub>O)<sub>0.5</sub>(CH<sub>3</sub>CN)(NO<sub>3</sub>)<sub>3</sub>] $\cdot$ CH<sub>3</sub>CN (Ln<sup>III</sup> = Dy **1** and Gd **2**), complemented with the magnetothermal studies of **2**. Previous results obtained by us and other authors on diphenoxo-bridged Ni<sup>II</sup>-Gd<sup>III</sup> complexes<sup>6,10g,l,n,p</sup> and 1,3-phenylendiimine bridged Ni<sup>II</sup>-Ni<sup>II</sup> complexes<sup>12</sup> have demonstrated that both types of bridges can transmit ferromagnetic interactions. Therefore, these compounds are expected to show ferromagnetic interactions between the metal ions and a high multiplicity in the ground state, which can favor the SMMs behavior in **1** and the existence of a large MCE in **2**. Furthermore, isostructural Ni<sub>2</sub>Y<sub>2</sub> complex containing diamagnetic Y<sup>III</sup> atoms was prepared to obtain information for the analysis of the magnetic properties of **1** and **2**.

## Experimental Section

**General Procedures:** Unless stated otherwise, all reactions were conducted in oven-dried glassware in aerobic conditions, with the reagents purchased commercially and used without further purification. The ligand H<sub>2</sub>L was prepared as previously described.<sup>13</sup>

### Preparation of complexes

[Dy<sub>2</sub>Ni<sub>2</sub>(NO<sub>3</sub>)<sub>6</sub>(H<sub>2</sub>O)<sub>1.5</sub>(CH<sub>3</sub>CN)<sub>2</sub>(L)<sub>2</sub>].CH<sub>3</sub>CN (**1**) (**Dy<sub>2</sub>Ni<sub>2</sub>**). To a solution of H<sub>2</sub>L (47.5 mg, 0.125 mmol) in 10 mL acetonitrile were subsequently added with continuous stirring 36.5 mg (0.125 mmol) of Ni(NO<sub>3</sub>)<sub>2</sub> · 6H<sub>2</sub>O and 56.5 mg (0.125 mmol) of Dy(NO<sub>3</sub>)<sub>3</sub> · 5H<sub>2</sub>O and 36 μL of triethylamine (0.25 mmol). The resulting yellow solution was filtered and allowed to stand at room temperature. After two days, well-formed prismatic crystals of compound **1** were obtained with yields of 55% based on Ni. Anal. Calc. For C<sub>50</sub>H<sub>48</sub>Dy<sub>2</sub>N<sub>13</sub>Ni<sub>2</sub>O<sub>27.5</sub>: C, 35.01; H, 2.82; N, 10.62. Found: C, 35.09; H, 2.75; N, 10.56 %. IR(KBr, cm<sup>-1</sup>): 3350 (m), 1612 (s), 1589 (s), 1560 (s), 1469 (vs), 1382 (vs), 1295(s), 975 (m), 740 (m)

[Gd<sub>2</sub>Ni<sub>2</sub>(NO<sub>3</sub>)<sub>6</sub>(H<sub>2</sub>O)<sub>1.5</sub>(CH<sub>3</sub>CN)<sub>2</sub>(L)<sub>2</sub>].CH<sub>3</sub>CN (**2**) (**Gd<sub>2</sub>Ni<sub>2</sub>**). This compound was prepared in a 60 % yield as green crystals following the procedure for **1**, except that Gd(NO<sub>3</sub>)<sub>3</sub> · 6H<sub>2</sub>O (59 mg, 0.125 mmol) was used instead of Dy(NO<sub>3</sub>)<sub>3</sub> · 5H<sub>2</sub>O. Anal. Calc. For C<sub>50</sub>H<sub>48</sub>Gd<sub>2</sub>N<sub>13</sub>Ni<sub>2</sub>O<sub>27.5</sub>: C, 35.25; H, 2.84; N, 10.70. Found: C, 35.11; H, 2.92; N, 10.79 %. IR(KBr, cm<sup>-1</sup>): 3350 (m), 1612 (s), 1589 (s), 1560 (s), 1469 (vs), 1382 (vs), 1297(s), 975 (m), 740 (m)

[Y<sub>2</sub>Ni<sub>2</sub>(NO<sub>3</sub>)<sub>6</sub>(H<sub>2</sub>O)<sub>1.5</sub>(CH<sub>3</sub>CN)<sub>2</sub>(L)<sub>2</sub>].CH<sub>3</sub>CN (**3**) (**Yb<sub>2</sub>Ni<sub>2</sub>**). This compound was prepared in a 60 % yield as green crystals following the procedure for **1**, except that Y(NO<sub>3</sub>)<sub>3</sub> · 6H<sub>2</sub>O (49.2 mg, 0.125 mmol) was used instead of Dy(NO<sub>3</sub>)<sub>3</sub> · 5H<sub>2</sub>O. Anal. Calc. For C<sub>50</sub>H<sub>48</sub>Y<sub>2</sub>N<sub>13</sub>Ni<sub>2</sub>O<sub>27.5</sub>: C, 38.34; H, 3.09; N, 11.62. Found: C, 38.21; H, 2.98;

N, 11.74 %. IR(KBr,  $\text{cm}^{-1}$ ): 3350 (m), 1612 (s), 1589 (s), 1560 (s), 1469 (vs), 1382 (vs), 1297(s), 975 (m), 740 (m)

### **Physical measurements**

Elemental analyses were carried out at the “Centro de Instrumentacion Cientifica” (University of Granada) on a Fisons-Carlo Erba analyser model EA 1108. IR spectra on powdered samples were recorded with a Thermo Nicolet IR200FTIR using KBr pellets.

### **Single-Crystal Structure Determination.**

Data were collected on Single crystals of **1** and **2** at 110 K using a Bruker AXS SMART APEX CCD diffractometer (Mo  $K\alpha$  radiation,  $\lambda = 0.71073 \text{ \AA}$ ) outfitted with a CCD area-detector and equipped with an Oxford Cryosystems 700 series Cryostream device. A data collection strategy using  $\omega$  and  $\varphi$  scans at 0.5 steps yielded full hemispherical data with excellent intensity statistics. Unit cell parameters were determined and refined on all observed reflections using APEX2 software.<sup>14</sup> Data reduction and correction for Lorentz polarization were performed using SAINT software.<sup>15</sup> Absorption corrections were applied using SADABS.<sup>16</sup> The structures were solved by direct methods and refined by the least squares method on  $F^2$  using the SHELX software suite<sup>17</sup> using Olex2 program.<sup>18</sup> All non-hydrogen atoms were refined anisotropically. Hydrogen atom positions were calculated and isotropically refined as riding models to their parent atoms. Summary of selected data collection and refinement parameter can be found from the Supporting Information (Table S1).

### **Magnetic Properties**

The variable temperature (2-300 K) magnetic susceptibility measurements under an applied field of 1000 Oe were carried out with a Quantum Design SQUID MPMS XL-5 device. *Ac* magnetic susceptibility measurements in the range 1-10000 Hz were carried

out with a Quantum Design Physical Property Measurement System (PPMS) using an oscillating *ac* field of 3.5 Oe. The experimental susceptibilities were corrected for the sample holder and diamagnetism of the constituent atoms by using Pascal's tables.

## Results and Discussion

H<sub>2</sub>L is a polydentate ligand with bis(NOO') donor atoms that can also act as a bridge between metal ions through both 1,3-phenylendiimine and phenolate groups. Former one can lead to the formation of Ni<sub>2</sub> metallacycles whereas latter can bridge the Ni<sup>II</sup> and Ln<sup>III</sup> ions. As expected, a reaction between H<sub>2</sub>L and Ni(NO<sub>3</sub>)<sub>2</sub>·6H<sub>2</sub>O in acetonitrile, followed by addition of Ln(NO<sub>3</sub>)<sub>3</sub>·5H<sub>2</sub>O and triethylamine while using a 1:1:1:2 molar ratio, afforded the tetranuclear Ni<sub>2</sub>Ln<sub>2</sub> complexes **1** and **2** in good yield.

Single-crystal X-ray diffraction studies reveal that compounds **1** and **2** are isostructural hence **1** will be used as a representative example to illustrate the common features of the two complexes. The molecular structure of **1** is shown in Figure 2, whereas comprehensive listing of bond lengths and angles for both **1** and **2** are given in the Supporting Information (Table S2).

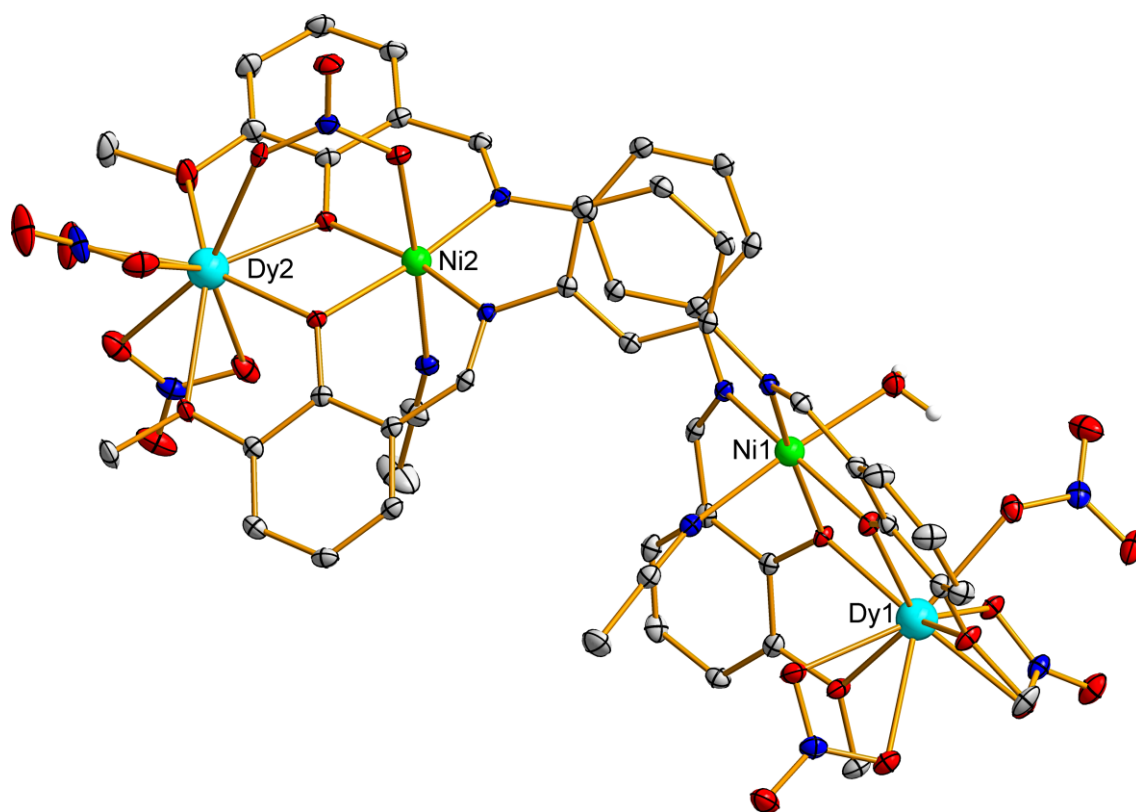


**Figure 2.** Perspective view of the structure of **1**. Only one of the disordered configurations is represented. Non-coordinated solvents molecules are omitted for clarity.

The solid state structure of **1** consists of  $[\text{Dy}_2\text{Ni}_2(\text{NO}_3)_6(\text{H}_2\text{O})_{1.5}(\text{CH}_3\text{CN})_2(\text{L})_2]$  molecules of  $C_1$  symmetry with acetonitrile as solvent of crystallization. The neutral tetranuclear unit can be described as a twelve-membered  $\text{Ni}_2$  metallacycle with di(*m*-phenylendiimine) bridges connected on both sides to  $\text{Dy}^{\text{III}}$  ions through diphenoxo-bridging groups. The structure is very similar to that previously reported for the complex  $\{[\text{SnBu}_2][\text{Ni}(\text{L})(\text{NCS})_2]\}$ .<sup>19</sup> The  $\text{Ni}^{\text{II}}$  ions exhibit distorted octahedral coordination environments, in which the equatorial plane is composed of two *cis*-imine nitrogens and two phenolato oxygens belonging to pair of fully deprotonated bis(tridentate)  $\text{L}^{2-}$  bridging ligands. The axial positions are occupied by the nitrogen atom of an acetonitrile and the oxygen atom of a coordinated water molecule. Around the  $\text{Ni}_2\text{-Dy}_2$  fragment the nitrate and water ligands are disordered in the way that one part of the disorder can be refined as a monodentately coordinated nitrate and water



molecule as in the Ni1-Dy1 unit, while the other part is formed by bridging nitrate anion (Figure S1). Hence, other axial position of Ni2 is occupied by either oxygen from the disordered water molecule or from the bidentate bridging nitrate. The occupation factor ratio between the two parts of the disorder refined very close to 0.5 and was thus fixed into that value (*i.e.* atoms in both parts are presented in the crystal with equal occupation of 0.5). The Ni-N<sub>imine</sub> and Ni-O<sub>phen</sub> bond distances are in the ranges 2.092-2.109 Å and 2.028-2.099 Å, respectively, whereas the Ni-N and N-O axial bond distances are 2.072 Å and 2.095 Å, and 2.078 Å and 2.110 Å, respectively.

The Dy1 atom exhibits a rather non-symmetrical DyO<sub>9</sub> coordination, which consists of two bridging phenoxo oxygens, two methoxy oxygens and five oxygen atoms belonging to two bidentate and one monodentate nitrate anions. The Dy2 atom exhibits similarly a DyO<sub>9</sub> coordination sphere, which is built, in addition to the phenoxo and methoxy oxygens from the ligand, of five oxygen atoms belonging to three coordinated nitrate anions (two bidentate and disordered bridging or monodentate one). In addition to the disorder involving the water molecule and bridging/monodentate nitrate anion (*vide supra*), both bidentately coordinated nitrates can be refined in distinct parts with slightly different terminal positions. The Dy-O<sub>phenoxo</sub> bond distances in the range of 2.342(2) Å and 2.322(2) Å are shorter than Dy-O<sub>nitrate</sub> and Dy-O<sub>methoxy</sub> bond lengths in the ranges 2.492(2)-2.522(2) Å and 2.608(2) Å-2.564(2) Å, respectively, thus indicating a high degree of asymmetry in the DyO<sub>9</sub> coordination spheres. In fact, the calculation of the degree of distortion of the Dy coordination polyhedra with respect to ideal nine-vertex, by using the continuous shape measure theory and SHAPE software,<sup>20</sup> indicated that the lower values of the shape measures were those relative to the, muffin (*C<sub>s</sub>*), spherical capped square antiprism (*C<sub>4v</sub>*), spherical tricapped trigonal prism (*D<sub>3h</sub>*) (1.90, 2.43 and 2.26, respectively, for Dy1, 2.35, 2.49 and 2.22, respectively, for Dy2

with the monodentate nitrate anion and 2.39, 3.03 and 4.06, respectively, for Dy2 with the bridging nitrate). Therefore, the DyO<sub>9</sub> coordination sphere can be considered as intermediate between all these nine-vertex polyhedra. The shape measures relative to other reference polyhedra are significantly larger (see table S3).

The Ni( $\mu$ -O<sub>2</sub>)Dy bridging fragments are almost planar with a hinge angles of 177.8(1) $^\circ$  and 172.1(1) $^\circ$  (dihedral angle between the O-Ni-O and O-Dy-O planes) for Dy1 and Dy2, respectively, and rather symmetric average Ni-O-Dy bridging angles of 105.1 $^\circ$  and 106.3 $^\circ$ . The Ni1 $\cdots$ Dy1 and Ni2 $\cdots$ Dy2 separations are 3.489(1) Å and 3.437(1) Å, whereas the Ni $\cdots$ Ni distance is 6.889(1) Å. The angles between the bridging phenylene rings and the NiN<sub>2</sub>O<sub>2</sub> equatorial coordination planes of Ni1 and Ni2 are 57.1 $^\circ$ , 66.0 $^\circ$  and 60.6 $^\circ$  and 69.7 $^\circ$ , respectively. The phenylene rings are rotated and slightly tilted each to other with an interplanar distance of 3.302 Å, thus indicating the existence of significant  $\pi\cdots\pi$  interactions.

In spite of a large interest in 3d/4f complexes only a few examples of tetranuclear Ni<sup>II</sup><sub>2</sub>Ln<sup>III</sup><sub>2</sub> complexes have been reported so far<sup>8j,q,21</sup> and to the best of our knowledge, complexes **1** and **2** represent the first reported examples of linear Ln<sup>III</sup>-Ni<sup>II</sup>-Ni<sup>II</sup>-Ln<sup>III</sup> species.

## Magnetic Properties

The magnetic properties of **1** and **2** were measured on polycrystalline samples in the 2-300 K temperature range under an applied magnetic field of 0.1 T and the data are given in Figure 3 in the form  $\chi_M T$  vs  $T$  (where  $\chi_M$  is the magnetic susceptibility per Ni<sup>II</sup><sub>2</sub>Ln<sup>III</sup><sub>2</sub> unit).

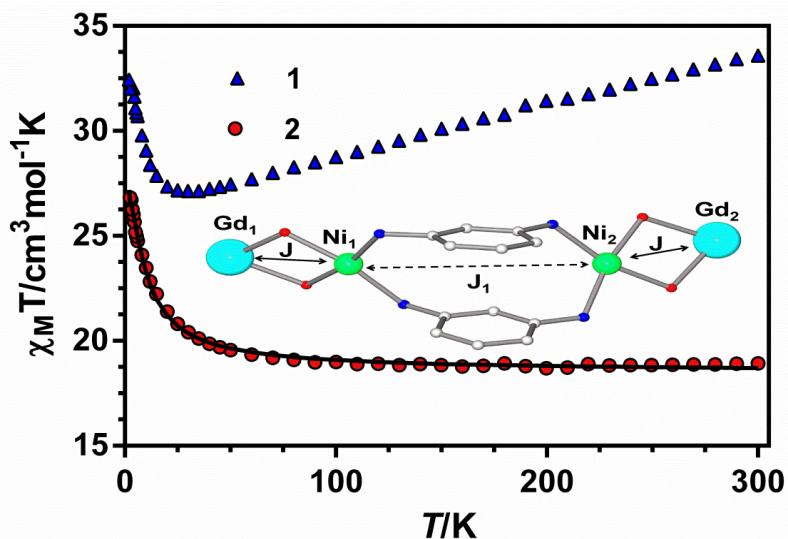


**Figure 3.** Temperature dependence of the  $\chi_M T$  for **1** and **2**. Solid line represents the best fit of the experimental data of **2** with the Hamiltonian in equation 1.

**Dy<sub>2</sub>Ni<sub>2</sub> (1).** At room temperature, the  $\chi_M T$  product of **1** ( $33.6 \text{ cm}^3 \text{ K mol}^{-1}$ ) is close to the calculated value for independent Ni<sup>II</sup> ( $S = 1$  with  $g_{\text{Ni}} = 2.0$ ) and Dy<sup>III</sup> ions ( ${}^6H_{15/2}$ ,  $g_{\text{Dy}} = 4/3$ ) in the free-ion approximation ( $30.34 \text{ cm}^3 \text{ K mol}^{-1}$ ). The  $\chi_M T$  value for **1** decreases slowly with decreasing temperature, reaching a minimum at  $\sim 30 \text{ K}$  with a value of  $27.14 \text{ cm}^3 \text{ K mol}^{-1}$ . This behavior is due to depopulation of the  $m_j$  sublevels of the Dy<sup>III</sup> ion, which arise from the splitting of the ground  ${}^6H_{15/2}$  multiplet by the ligand field. Below the temperature of the minimum,  $\chi_M T$  increases to reach a value of  $32.44 \text{ cm}^3 \text{ K mol}^{-1}$  at  $2 \text{ K}$ . The increase in  $\chi_M T$  below  $\sim 30 \text{ K}$  is due to a ferromagnetic interaction between Ni<sup>II</sup> and Dy<sup>III</sup>.

The  $M$  versus  $H$  plot at  $2 \text{ K}$  for **1** (Figure S2) shows a relatively rapid increase in the magnetization at low field in accord with a high-spin state for this complex and then a linear increase without achieving a complete saturation at  $5 \text{ T}$ . The linear high-field variation of the magnetization suggests the presence of a significant magnetic anisotropy and/or low-lying excited states that are partially populated. It should be noted that the magnetization value for **1** at  $5 \text{ T}$  ( $14.35 \text{ N}\mu_{\text{B}}$ ) are far from the saturation

values expected for two Dy<sup>III</sup> ions ferromagnetically coupled with two  $S_{\text{Ni}} = 1$  ( $24 N\mu_{\text{B}}$ ), which is due to the splitting of the ground multiplet of the Dy<sup>III</sup> ion promoted by the crystal-field effects (the saturation magnetization for mononuclear Dy<sup>III</sup> complexes is  $\sim 5 N\mu_{\text{B}}$ ).<sup>22</sup>

Dynamic *ac* magnetic susceptibility measurements as a function of the temperature and frequency for **1** are given in Figure 4 and Figure S3, respectively. Dynamic *ac* magnetic susceptibility measurements as a function of the temperature under zero-external applied *dc* field show a frequency dependency of the in-phase ( $\chi'_{\text{M}}$ ) and out-of-phase ( $\chi''_{\text{M}}$ ) signals (Figure 4). This behavior seems to indicate slow relaxation of the magnetization, as typical of a SMM. However, there is not any clear maximum in the temperature dependence of  $\chi''_{\text{M}}$  above 2 K, at frequencies reaching 10000 Hz. This feature could be due either to the existence of fast resonant zero-field quantum tunneling of the magnetization (QTM) through degenerate energy levels or to a very small energy barrier. The QTM relaxation process is forbidden for Kramers doublets (the zero-field tunnel splitting is zero), but could be turned on by dipolar and/or hyperfine interactions. When the *ac* measurements were performed in the presence of a small external *dc* field of 1000 G to fully or partly suppress the quantum tunneling relaxation, compound **1** showed slow relaxation of the magnetization with clear maxima in the  $\chi''_{\text{M}}$  vs  $T$  curves, which appear in the 2.0 K (1000Hz)-2.61 K (10000 Hz) range (Figure 4).

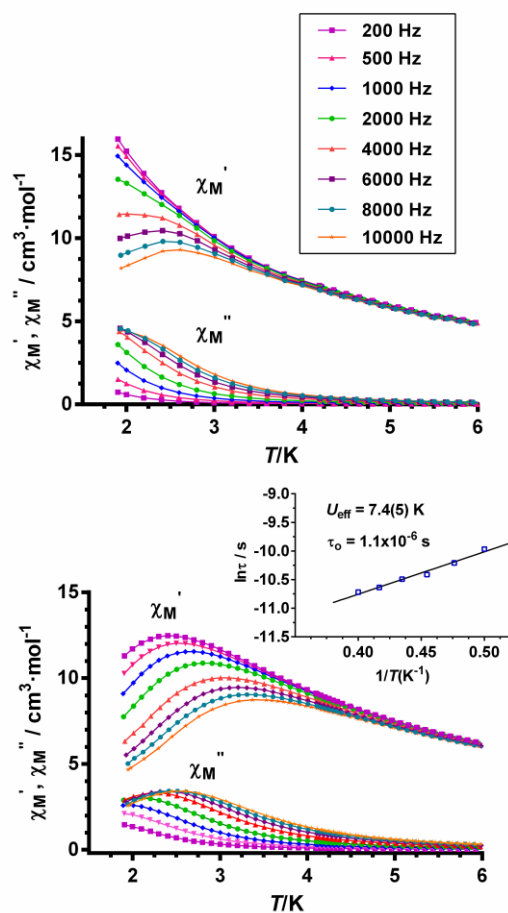


**Figure 4.** In-phase ( $\chi'_{M}$ ) and out-of-phase ( $\chi''_{M}$ ) signals under zero (top) and 1000 Oe (bottom) *dc* fields and Arrhenius plot (inset) for **1**.

The Cole-Cole diagrams in the temperature range 2-2.8 K (Figure S4) exhibit semicircular shapes and can be fitted using the generalized Debye model, affording  $\alpha$  values in the range 0.23-0.37, which supports the existence of a broad distribution of relaxation times. The set  $\chi_0$  (isothermal susceptibility),  $\chi_s$  (adiabatic susceptibility) and  $\alpha$  obtained in the above fits were further used to fit the frequency dependence of  $\chi''_{M}$  at each temperature to the generalized Debye model, which permits the relaxation time  $\tau$  to be extracted. The results were then used in constructing the Arrhenius plot shown in Figure 4. The linear fit of the data ( $\tau$  vs  $1/T$ ) afforded an effective energy barrier for the reversal of the magnetization of  $U_{\text{eff}} = 7.4(5)$  K with  $\tau_0 = 1.1 \times 10^{-6}$  s. The fact that the isostructural  $\text{Ni}_2\text{Y}_2$  complex does

not exhibit slow relaxation of the magnetization above 2 K, points out that the SMM behavior found for **1** arises from the presence of the Dy<sup>III</sup> ions.

It should be noted at this point that Ln<sup>III</sup>-Ni<sup>II</sup> polynuclear complexes are attracting much attention in the field of SMMs, because the combination of Ln<sup>III</sup> ions with strong magnetic anisotropic and Ni<sup>II</sup> ions with second-order magnetic anisotropy could lead to improved SMMs properties. In spite of this, only a few examples of Ni-Ln complexes (with paramagnetic Ni<sup>II</sup> ions) exhibiting SMMs have been reported so far.<sup>6,10</sup> Most part of them are field-induced SMMs and, as far as we know, only in six instances SMM behaviour was observed under zero-field with maxima in the *ac* out-of-phase peaks above 2 K.<sup>10a</sup>, which exhibit relatively small energy barriers. Among them, the defective cubane complexes Ni<sub>4</sub>Ln<sub>2</sub> (Ln<sup>III</sup> = Tb, Dy) present the highest thermal energy barriers reported so far with  $U_{\text{eff}}$  values of 30 K and 32 K, respectively.<sup>10a</sup> The small energy barrier observed for **1** and other Ni-Dy based SMMs could be due, among other reasons, to: (i) a weak anisotropy for the whole molecule and (ii) the weak magnetic exchange coupling between Ni<sup>II</sup> and Dy<sup>III</sup> ions, leading to a small energy separation between the ground and first excited state, which determine the value of  $U_{\text{eff}}$ . As for point (i), either a small anisotropy of the Dy<sup>III</sup> ions induced by the ligand-field effects or the different relative orientation of the local anisotropic axes of the Ni<sup>II</sup> and Dy<sup>III</sup> ions could lead to a relatively weak anisotropy of the whole molecule. As for point (ii), the Ni-Dy interactions generally are weaker than the Ni-Gd ones and therefore a  $J_{\text{NiDy}} < 2$  cm<sup>-1</sup> is expected for **1** (see below). For such a  $J$  value the first excited state is of only a few wavenumbers above the ground state and therefore the thermal energy barrier would be small. Additionally, because the Ni-Dy interaction is weak, the Ni<sup>II</sup> ions can have independently reorienting magnetic moments at  $T = 2$  K, so that they are sources of a random magnetic field for the Dy<sup>III</sup> ion, thus favoring a quantum tunneling splitting

that diminishes the thermal energy barrier.<sup>23</sup> The fact that the Ni<sub>3</sub>Dy<sub>2</sub> pentanuclear complex recently reported by Chadrasekhar et al,<sup>24</sup> in which the Ni<sup>II</sup> are diamagnetic, exhibits the highest energy barrier ever found for a Ni-Dy system ( $U_{\text{eff}} = 85$  K), supports our hypothesis that weak Dy-Ni interactions lead to a small gap between the ground and first excited states and then to small energy barriers. In good accord with this hypothesis, the N<sub>2</sub><sup>3-</sup> radical bridged dinuclear complex, [K(18-crown-6)]{[(Me<sub>3</sub>Si)<sub>2</sub>N]<sub>2</sub>(THF)Dy}<sub>2</sub>( $\mu$ - $\eta^2$ : $\eta^2$ -N<sub>2</sub>),<sup>25</sup> with a very important magnetic exchange interaction between the radical and the Dy<sup>III</sup> ions, exhibits a very large anisotropy barrier ( $U_{\text{eff}} = -123$  cm<sup>-1</sup>). However, the non-radical N<sub>2</sub><sup>2-</sup>-bridged analogue,<sup>25</sup> with a very weak magnetic exchange interaction between the Dy<sup>III</sup>, shows a drastic reduction of the anisotropy barrier to  $U_{\text{eff}} = 18$  cm<sup>-1</sup>. These results highlight the essential role played by the magnetic exchange interaction in determining the magnitude of the anisotropy barrier in lanthanide containing polynuclear complexes.

In view of the above considerations, the approach of introducing several anisotropic metal ions in a polynuclear complex, as in **1**, may not have a positive effect on the SMM behavior. In connection with this, Chibotaru *et al.*<sup>26</sup> have recently suggested from theoretical studies that a better strategy to obtain efficient SMMs systems would be that of combining strong anisotropic metal ions with large angular momentum and isotropic metal ions with large spin momentum, such as Gd<sup>III</sup>.

**Gd<sub>2</sub>Ni<sub>2</sub> (2).** The room-temperature  $\chi_{\text{M}}T$  value for **2** of 18.92 cm<sup>3</sup> K mol<sup>-1</sup> is slightly higher but still in relative good agreement with the expected value for a couple of Ni<sup>II</sup> ( $S = 1$ ) and a couple Gd<sup>III</sup> ( $S = 7/2$ ) non-interacting ions (17.75 cm<sup>3</sup> K mol<sup>-1</sup> with  $g = 2$ ). On lowering the temperature, the  $\chi_{\text{M}}T$  slowly increases from room temperature to 50 K (19.55 cm<sup>3</sup> K mol<sup>-1</sup>) and then in a more abrupt way to reach a value of 26.82 cm<sup>3</sup> K mol<sup>-1</sup> at 2.5 K (Figure 3). This behavior is due to Ni<sup>II</sup>-Gd<sup>III</sup> and Ni<sup>II</sup>-Ni<sup>II</sup> ferromagnetic

interactions through the diphenoxo and diphenylenediimine bridging groups leading to a  $S_T = 9$  ground spin state.<sup>21</sup> The magnetic properties of **2** have been modelled by using the following Hamiltonian:

$$\hat{H} = -J(\hat{S}_{Ni1}\hat{S}_{Gd1} + \hat{S}_{Ni2}\hat{S}_{Gd2}) - J_1(\hat{S}_{Ni1}\hat{S}_{Ni2}) + D_{Ni} \sum_{i=1}^2 (\hat{S}_{zi}^2 - S_i(S_i + 1)/3) \quad (\text{eq. 1})$$

where  $J$  and  $J_1$  account for the magnetic exchange coupling between Ni<sup>II</sup> and Gd<sup>III</sup> ions through the diphenoxo bridging group and between the Ni<sup>II</sup> ions, through the diphenylenediimine bridging group, respectively, and  $D_{Ni1}$  and  $D_{Ni2}$  are the axial single ion zero-field splitting parameters of the Ni<sup>II</sup> ions. Although there are small differences between the bond angles and distances affecting the two halves of the molecule, for the sake of simplicity, we are going to consider the same exchange coupling for the two Ni<sup>II</sup>-Gd<sup>III</sup> interactions. It should be noted that  $J_1$  and  $D$  are correlated, so that  $D$  increases as does  $J_1$ . In view of this, we decided to study the magnetic properties (Figure S5) of the isostructural Ni<sub>2</sub>Y<sub>2</sub> complex (**3**) to get an estimate of the zero-field splitting parameter  $D$  and to confirm the nature of the magnetic exchange interaction mediated by the phenylenediimine bridge ( $J_1$ ). It should be noted that even though we have not been able to obtain single crystals of **3** of high enough quality to determine the molecular structure, elemental analyses, IR spectra and powder X-ray diffraction data clearly indicate that all three complexes are isostructural (Figure S6 and S7). The  $\chi_M T$  product for **3** at room temperature (2.17 cm<sup>3</sup> K mol<sup>-1</sup>) is close to that expected for two non-interacting Ni<sup>II</sup> ions with  $g = 2$  of 2.0 cm<sup>3</sup> K mol<sup>-1</sup>). On lowering the temperature, the  $\chi_M T$  product slowly increases with decreasing temperature from 300 to 15 K (2.195 cm<sup>3</sup> K mol<sup>-1</sup>) and then drop sharply to 1.40 cm<sup>3</sup> K mol<sup>-1</sup> at 2 K. The increase in the 300-15 K temperature range is due to a very weak ferromagnetic interaction between the Ni<sup>II</sup>, whereas the decrease at low temperature can be due to different factors, such as, the existence of intermolecular antiferromagnetic interactions between Ni<sub>2</sub>Y<sub>2</sub> and zero-



field splitting effects of the Ni<sup>II</sup> ions. As the molecules are well isolated in the crystal, we believe that the decrease in  $\chi_{\text{M}}T$  at low temperature is mainly due to the latter factor. Hence, we have modelled the magnetic properties of **3** with the following Hamiltonian

$$\hat{H} = -J_1(\hat{S}_{\text{Ni}1}\hat{S}_{\text{Ni}2}) + D_{\text{Ni}} \sum_{i=1}^2 (\hat{S}_{zi}^2 - S_i(S_i + 1)/3) \quad (\text{eq. 2})$$

where  $J_1$  and  $D_{\text{Ni}}$  account for the magnetic exchange coupling between Ni<sup>II</sup> ions and the axial single ion zero-field splitting parameter of the Ni<sup>II</sup> ion, respectively. Simultaneous fitting of the  $\chi_{\text{M}}T$  versus  $T$  and the  $M$  versus field at 2 K with the above Hamiltonian with the PHI program (using a mean  $g$  value to avoid overparametrization) afforded the following set of parameters:  $J_1 = +0.38 \text{ cm}^{-1}$ ,  $g = 2.08$ ,  $D_{\text{Ni}} = 4.63 \text{ cm}^{-1}$  and  $R = 1.5 \times 10^{-6}$  ( $R = \sum (\chi_{\text{M}}T_{\text{calc}} - \chi_{\text{M}}T_{\text{exp}})^2 / \sum (\chi_{\text{M}}T_{\text{exp}})^2$ ). The  $D_{\text{Ni}}$  values are in agreement with the expected single-ion values reported in the literature.<sup>27</sup>

The  $D_{\text{Ni}}$  value extracted for compound **3** was used as a fixed parameter in the fitting of the magnetic data of **2** with the Hamiltonian given in equation 1. The simultaneous fitting of the  $\chi_{\text{M}}T$  vs  $T$  (Figure 3) and the  $M$  vs field plots (Figure 5) allowed to extract the following parameters:  $J = +1.80 \text{ cm}^{-1}$ ,  $J_1 = +0.42 \text{ cm}^{-1}$ ,  $g = 2.04$  and  $R = 4.2 \times 10^{-5}$  (with a fixed  $D = 4.63 \text{ cm}^{-1}$ ). When  $D$  is fixed to zero, the same values are obtained for  $J$  and  $g$ , but  $J_1$  decreases to a value of  $+0.23 \text{ cm}^{-1}$  with  $R = 4.3 \times 10^{-5}$ .

Theoretical calculations carried out on diphenoxo bridged NiGd<sup>2b,6,28</sup> complexes have shown that the ferromagnetic interaction between the Ni<sup>II</sup> and Gd<sup>III</sup> ions increases with the increase of  $\theta$  (Ni-O-Gd bridging angle) and with the decrease of  $\beta$  (the hinge dihedral angle between the O-Ni-O and O-Gd-O planes), although the former angle plays a major role in determining the value of  $J$ . The experimental  $J$  values for diphenoxo-bridged Ni-Gd dinuclear complexes given in Table 1 are in good accord with these magneto-structural correlations. As can be observed in this table, Ni-Gd

complexes having structural parameters similar to those of **2**, that is to say, almost planar systems ( $\beta \sim 0$ ) and  $\theta$  angles of  $\sim 106^\circ$ , present  $J$  values of  $\sim +2 \text{ cm}^{-1}$ , which are very close to that found for **2**.

**Table 1:** Magneto-structural data for diphenoxo bridged dinuclear NiGd complexes.

Complex	$J_{\text{exp}}(\text{cm}^{-1})$	$\theta$ ( $^\circ$ ) <sup>a</sup>	$\beta$ ( $^\circ$ ) <sup>a</sup>	Gd...Ni ( $\text{\AA}$ ) <sup>a</sup>	Ref.
$[\text{Ni}(\text{H}_2\text{O})(\mu\text{-L}^1)\text{Ln}(\text{NO}_3)_3] \cdot 2\text{CH}_3\text{OH}$	+2.16	109.4	2.3	3.565	6
$[\text{L}^2\text{Ni}(\text{H}_2\text{O})_2\text{Gd}(\text{NO}_3)_3]$	+3.6	107.2	2.8	3.522	10a
$[\text{Ni}(\text{CH}_3\text{CN})_2(\text{valpan})\text{Gd}(\text{NO}_3)_3] \cdot \text{CH}_3\text{CN}$	+2.3	106.1	0.22	3.467	10g
$[\text{Ni}(\mu\text{-L}^1)(\mu\text{-Ac})\text{Gd}(\text{NO}_3)_2]$	+1.38	104.4	21.4	3.456	6
$[\text{Ni}(\text{valpan})(\text{MeOH})(\text{ac})\text{Ln}(\text{hfac})_2]$	+2.2	102.1	13.5	3.384	10l
$[(\text{H}_2\text{O})\text{Ni}(\text{ovan})_2(\mu\text{-NO}_3)\text{Gd}(\text{ovan})(\text{NO}_3)_2]\text{H}_2\text{O}$	+1.36 <sup>b</sup>	101.6	0.8	3.324	10e
$[\text{L}^3\text{Ni}(\text{H}_2\text{O})(\mu\text{-OAc})\text{Ln}(\text{NO}_3)_2] \cdot \text{CH}_3\text{CN}$	+1.54	103.3	14.8	3.443	10n

<sup>a</sup> average values; <sup>b</sup>There are two  $J_{\text{NiGd}}$  as the  $\text{GdNi}_2$  trinuclear complex is not centrosymmetric; <sup>b</sup>No available structural data and those included in the table correspond to the  $\text{YNi}_2$  isostructural complex;  $\text{H}_2\text{L}^1 = N,N',N''\text{-trimethyl-}N,N''\text{-bis(2-hydroxy-3-methoxy-5-methylbenzyl)diethylenetriamine}$   $\text{H}_2\text{L}^2 = N,N\text{-2,2-dimethylpropylenedi(3-methoxysalicylideneiminato)}$ ; valpan =  $N,N\text{-propylenedi (3-methoxysalicylideneiminato)}$ ; ovan = *o*-vanillin;  $\text{H}_2\text{L}^3 =$  Schiff-base resulting from the 1:2 condensation of 1,1'-diacetylferrocene dihydrazone.  $\theta$  is the Ni-O-Gd bridging angle and  $\beta$  is the dihedral angle between the O-Ni-O and O-Ln-O planes in the bridging fragment.

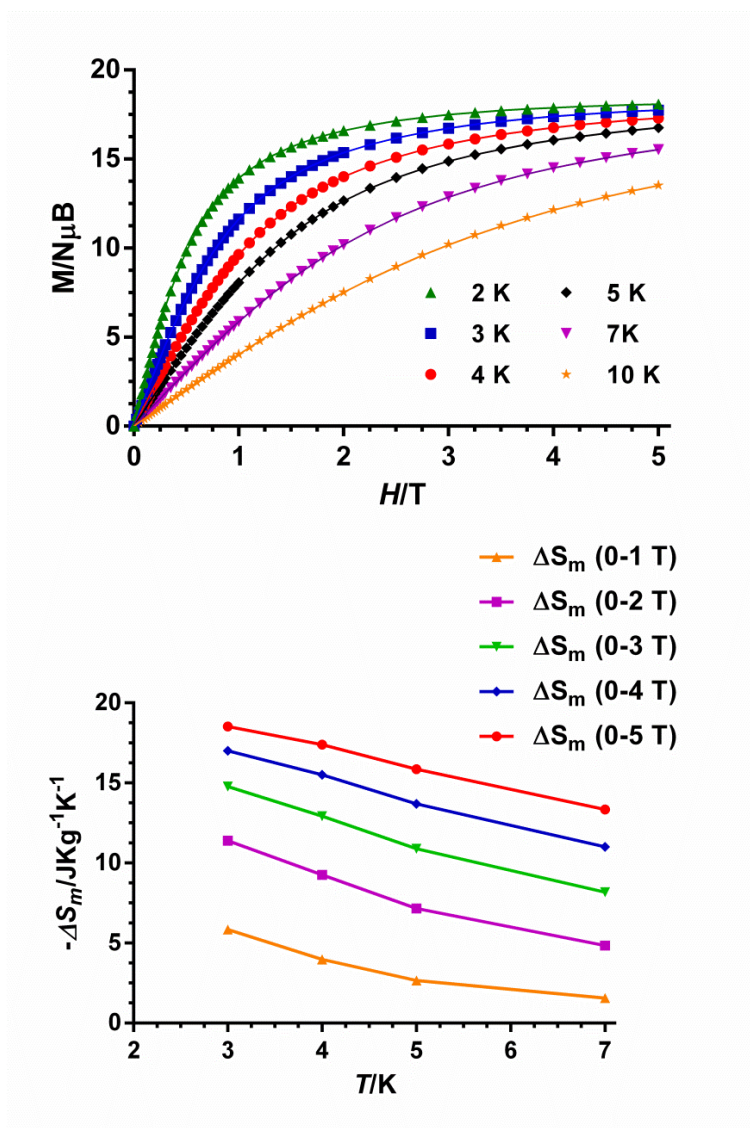


**Figure 5.**—The field dependence of the magnetization plots for **2** between 2 and 10 K (top) and magnetic entropy changes ( $-\Delta S_m$ ) calculated using the magnetization data for **2** from 1 to 5 T and temperatures from 3 to 7 K (bottom).

As far as we know, no examples of magnetically characterized Ni<sup>II</sup> dinuclear complexes with Schiff base ligands containing 1,3-phenylenediimine bridging fragment have been reported so far. However, results for dinuclear Cu<sub>2</sub> complexes with this type of ligands show ferromagnetic interactions and in one instance antiferromagnetic coupling.<sup>13,29</sup> It has been proposed that the nature and magnitude of the magnetic coupling depends on the substituents attached to the backbone of the ligand.<sup>29</sup> Interestingly, triple stranded Ni<sub>2</sub> complexes with 1,3-bis(pyridine-2-

carboxamide)benzene bearing the 1,3-phenylenediamine bridging fragment exhibit weak ferromagnetic interactions.<sup>12b-c</sup> In view of the above reported results, it would be reasonable to assume that the  $J_{\text{NiNi}}$  interaction through the 1,3-phenylenediimine bridging fragment should be ferromagnetic in nature. Nevertheless, in order to support the experimental values of the  $J_{\text{NiGd}}$  and fundamentally the ferromagnetic nature of the  $J_{\text{NiNi}}$  interaction through the 1,3-phenylenediimine bridging fragment, we have performed DFT calculations on the X-ray structures as found in solid state. The calculated  $J_{\text{Ni1Gd1}}$  and  $J_{\text{Ni2Gd2}}$  (structural parameters for both halves of the molecule are slightly different) are 3.39 and 3.33  $\text{cm}^{-1}$ , respectively, whereas the calculated  $J_{\text{Ni2Ni2}}$  is 1.35  $\text{cm}^{-1}$ , which agree in sign and rather well in magnitude with the corresponding experimental parameters. The difference between the experimental and calculated values could be due to limitations inherent to the method as well as to the fact that the experimental  $J$  values include the  $\text{Gd}_2\text{-Ni}_1$ ,  $\text{Gd}_1\text{-Ni}_2$  and  $\text{Gd}_1\text{-Gd}_2$  coupling constants, which have been calculated to be antiferromagnetic in nature with non-negligible  $J$  values of -0.44, -0.58 and -0.12  $\text{cm}^{-1}$ , respectively.

The magnetothermal properties of **2** were studied since the observed ferromagnetic interactions between the  $\text{Gd}^{\text{III}}$  and  $\text{Ni}^{\text{II}}$  ions and between the  $\text{Ni}^{\text{II}}$  ions induce a large total spin ground state ( $S = 9$ ) but also because  $\text{Gd}^{\text{III}}$  ions are isotropic and  $\text{Ni}^{\text{II}}$ , although anisotropic, possess only second order anisotropy. Therefore, a relatively significant magnetocaloric effect is expected for **2**. The magnetic entropy changes ( $-\Delta S_m$ ) that characterize the magnetocaloric properties of **2** can be calculated from the experimental isothermal field-dependent magnetization data (Figure 5) by using the Maxwell relation:

$$\Delta S_m(T, \Delta B) = \int_{B_i}^{B_f} \left[ \frac{\partial M(T, B)}{\partial T} \right]_B dB$$

where  $B_i$  and  $B_f$  are the initial and final applied magnetic fields. The values of  $-\Delta S_m$  for **2** under all fields increase as the temperature decreases from 7 to 3 K. The maximum value of  $-\Delta S_m$  achieved for **2** is  $18.5 \text{ J kg}^{-1} \text{ K}^{-1}$  at  $T = 3 \text{ K}$  with applied field change  $\Delta B = 5 \text{ T}$  (Figure 5). In spite of the  $\text{Ni}^{\text{II}}$  anisotropy, there is significant change in the  $-\Delta S_m$  for **2**, which is consistent with the easy spin polarization at relatively low magnetic field. It should be noted that  $-\Delta S_m$  could not be determined below 2 K due to limitations of our instrument, though it is expected to increase further with decreasing temperature. We have also simulated the MCE for **2**, using the magnetic parameters extracted when  $D$  was fixed to zero (see Figure S8). The obtained magnetic anisotropy values indicate that  $-\Delta S_m$  at 5 T is reduced in  $1.2 \text{ J kg}^{-1} \text{ K}^{-1}$  (5.7 %) by the  $\text{Ni}^{\text{II}}$  anisotropy.

As expected, the extracted  $-\Delta S_m$  value of  $18.5 \text{ J kg}^{-1} \text{ K}^{-1}$  at  $T = 3 \text{ K}$  is lower than that calculated for the full magnetic entropy content per mole, i.e.  $2R\ln(2S_{\text{Ni}} + 1) + 2R\ln(2S_{\text{Gd}} + 1) = 6.36 R = 31.08 \text{ J kg}^{-1} \text{ K}^{-1}$ , but it is higher than that expected for a  $S = 9 \text{ Ni}_2\text{Gd}_2$  unit, i.e.  $-\Delta S_m = R\ln(2S+1) = 2.94 R = 13.85 \text{ J kg}^{-1} \text{ K}^{-1}$ . Moreover, the extracted  $-\Delta S_m$  value at 5 T is larger than those observed for  $\text{Ni}_2\text{Gd}_2^{11\text{d}}$  and  $\text{Ni}_2\text{Gd}^{11\text{i,h}}$  complexes having similar molecular mass, but lower than those found under the same conditions for other more magnetic dense NiGd clusters with Gd/Ni ratios larger than 1<sup>11b,c,d</sup> and other  $\text{Gd}^{30}$  and 3d-Gd complexes<sup>31</sup>. However, the magnetothermal results for **2** and other small clusters demonstrate that these systems can be a good approach for novel molecular magnetic refrigerants.

### Concluding remarks

The multidentate ligand  $N,N'$ -bis(3-methoxysalicylidene)-1,3-diaminobenzene, with two sets of symmetrically distributed NO and OO' coordination pockets flanking the phenyl ring, shows selective preference for  $\text{Ni}^{\text{II}}$  and  $\text{Ln}^{\text{III}}$  ions, respectively, in the preparation of the first examples of structurally and magnetically characterized linear

tetranuclear  $\text{Ln}^{\text{III}}\text{-Ni}^{\text{II}}\text{-Ni}^{\text{II}}\text{-Ln}^{\text{III}}$  ( $\text{Ln}^{\text{III}} = \text{Dy } \mathbf{1}, \text{Gd } \mathbf{2}$ ) species. The central body of the complexes consists of a twelve-membered  $\text{Ni}_2$  metallacycle with di(*m*-phenylenediimine) bridges. On both sides of the ring,  $\text{Dy}^{\text{III}}$  ions are connected to  $\text{Ni}^{\text{II}}$  ions through diphenoxo-bridging groups. *Dc* magnetic susceptibility studies indicate the presence of dominant ferromagnetic interactions in both **1** and **2**. Complex **1** shows frequency-dependent out-of-phase *ac* signals, which is indicative of slow relaxation of the magnetization and potential SMM behavior, whereas complex **2** exhibits a  $S = 9$  ground state and significant MCE. Moreover, the reduction of the MCE effect promoted by the  $\text{Ni}^{\text{II}}$  anisotropy has been quantified to be of approximately a six percent. Currently, we are studying the structurally similar tetranuclear  $\text{M}_2^{\text{II}}\text{Ln}^{\text{III}}$  ( $\text{M}^{\text{II}} = \text{Co}, \text{Cu}, \text{Zn}$ ) complexes with the prospect of evaluating how the anisotropy of the metal ions or the presence of diamagnetic metal ions affect the SMM and magnetothermal properties. We expect that replacement of  $\text{Ni}^{\text{II}}$  by diamagnetic  $\text{Zn}^{\text{II}}$  in these  $\text{M}_2^{\text{II}}\text{Dy}^{\text{III}}$  complexes provokes a considerable increase of the effective energy barrier ( $U_{\text{eff}}$ ).

## ASSOCIATED CONTENT

X-ray crystallographic data for **1-2**, including data collection, refinement and selected bond lengths and angles. Shape measures, IR and PXRD data for **1-3**, *dc* susceptibility data for complex **3**, variable-frequency temperature dependence of the *ac* in-phase  $\chi'_{\text{M}}$  signal and Cole-Cole plots for complexes **1** and simulation of the MCE effect for **2** with  $D = 0$ . This material is available free of charge via the Internet at <http://pubs.asc.org>.

## AUTHOR INFORMATION

### Corresponding Author

\*Email: [ecolacio@ugr.es](mailto:ecolacio@ugr.es)

## Notes

The authors declare no competing financial interest.

## ACKNOWLEDGMENT

Financial support from Ministerio de Economía y Competitividad (MINECO) for Projects CTQ-2011-24478 and MAT2012-38318-C03-01, the Junta de Andalucía (FQM-195 and the Project of excellence P11-FQM-7756), and the University of Granada are acknowledged. S. T. thanks to Junta de Andalucía for a postdoctoral contract.

## References

- (1) For some recent reviews see: (a) Winpenny, R. E. P. *Chem. Soc. Rev.* **1998**, *27*, 447-452. (b) Benelli, C.; Gatteschi, D. *Chem. Rev.* **2002**, *102*, 2369-2388. (c) Sessoli, R.; Powell, A. K. *Coord. Chem. Rev.* **2009**, *253*, 2328-2341. (d) Andruh, M.; Costes, J. P.; Diaz C.; Gao, S. *Inorg.Chem.* **2009**, *48*, 3342-3359 (Forum Article). (e) “Molecular Magnets”, themed issue (Brechtin, E. K. Ed.), *Dalton Trans.* **2010**. (f) Andruh, M. *Chem. Commun.* **2011**, *47*, 3015. (g) Sorace, L.; Benelli, C.; Gatteschi, D. *Chem. Soc. Rev.* **2011**, *40*, 3092-3104.
- (2) Some reviews: (a) Evangelisti, M.; Brechin, E. K. *Dalton Trans.* **2010**, *39*, 4672-4676. (b) Cremades, E.; Gomez-Coca, S.; Aravena, D.; Alvarez, S.; Ruiz, E. *J. Am. Chem. Soc.* **2012**, *134*, 10532-10542. (c) Sharples J. W.; Collison, D. *Polyhedron* **2013**, *54*, 91-103. (d) Zheng, Y.-Z.; Zhou, G.-J.; Zheng, Z.; Winpenny, R. E. P. *Chem. Soc. Rev.* **2014**, *43*, 1462-1475.
- (3) Gatteschi, D.; Sessoli, R.; Villain, J. *Molecular Nanomagnets*. Oxford University Press. Oxford, UK, **2006**.

- (4) (a) Leuenerger, M. N.; Loss, D. *Nature*, **2001**, *410*, 789-793. (b) Rocha, A. R.; García-Suárez, V.M.; Bailey, S.W.; Lambert, C. J.; Ferrerand, J.; Sanvito, S. *Nat. Mater.* **2005**, *4*, 335-339. (c) Ardavan, A.; Rival, O.; Morton, J. J. L.; Blundell, S. J.; Tyryshkin, A. M.; Timco, G. A.; Winpenny, R. E. P. *Phys. Rev. Lett.*, **2007**, *98*, 057201. (d) Bogani L.; Wernsdorfer, W. *Nat. Mater.* **2008**, *7*, 179-186. (e) Affronte, M. *J. Mater. Chem.* **2009**, *19*, 1731-1737. (f) Stamp, P. C. E.; Gaita-Ariño, A. *J. Mater. Chem.* **2009**, *19*, 1718-1730. (g) Candini, A.; Klyatskaya, S.; Ruben, M.; Wernsdorfer, W.; Affronte, M. *Nano Lett.* **2011**, *11*, 2634-2639. (h) Vincent, R.; Klyatskaya, S.; Ruben, M.; Wernsdorfer, W.; Balestro, F. *Nature* **2012**, *488*, 357-360. (i) Ganzhorn, M.; Klyatskaya, S.; Ruben M.; Wernsdorfer, W. *Nature Nanotech.* **2013**, *8*, 165-169. (j) Jenkins, M.; Hümmel, T.; Marínez-Pérez, M. J.; García-Ripoll, J.; Zueco, D.; Luis, F. *New. J. Physics*, **2013**, *15*, 095007.
- (5) Sessoli, R. *Angew. Chem., Int. Ed.*, **2011**, *50*, 2.
- (6) Colacio, E.; Ruiz, J.; Mota, A. J.; Palacios, M. A.; Cremades, E.; Ruiz, E.; White, F. J.; Brechin, E. K. *Inorg. Chem.* **2012**, *51*, 5857-5868.
- (7) Colacio, E.; Ruiz, J.; Lorusso, G.; Brechin, E.K.; Evangelisti, M. *Chem. Commun.* **2013**, *49*, 3845-3847.
- (8) Martínez-Pérez, M.-J.; Montero, O.; Evangelisti, M.; Luis, F., Sesé, J.; Cardona-Serra, S.; Coronado, E., *Adv. Mater.* **2012**, *24*, 4301; (b) Martínez-Pérez, M.-J.; Cardona-Serra, S.; Schlegel, C.; Moro, F.; Alonso, P. J. ; Prima-García, H.; Clemente-Juan, J. M. , Evangelisti, M. ; Gaita-Ariño, A. ; Sesé, J.; van Slageren, J. ; Coronado, E.; Luis, F. , *Phys. Rev. Lett.* **2012**, *108*, 247213; (c) Baldoví, J. J.; Cardona-Serra, S.; Clemente-Juan, J. M.; Coronado, E.; Gaita-Ariño, A.; Prima-García, H. *Chem. Commun.*, **2013**, *49*, 8922.



- (9) Luis F.; Evangelisti, M., “*Magnetic refrigeration and spin-lattice relaxation in gadolinium-based molecular nanomagnets*”, in “*Molecular Nanomagnets and Related Phenomena*”, S. Gao (ed.), Springer-Verlag, Berlin, Heidelberg, (2014).
- (10) (a) Costes, J.-P.; Dahan, F.; Dupuis, A.; Laurent, J. P., *Inorg. Chem.* **1997**, *36*, 4284-4286. (b) Chen, Q.-Y.; Luo, Q.-H.; Zheng, L.-M.; Wang, Z.-L.; Chen, J.-T. *Inorg. Chem.* **2002**, *41*, 605-609. (c) Mori, F.; Ishida, T.; Nogami, T. *Polyhedron* **2005**, *24*, 2588-2592. (d) Yamaguchi, T.; Sunatsuki, Y.; Ishida, H.; Kojima, M.; Akashi, H.; Re, N.; Matsumoto, N.; Pochaba, A.; Mrozinski, J. *Inorg. Chem.* **2008**, *47*, 5736-5745. (e) Costes J.-P.; Vendier L. *Eur. J. Inorg. Chem.* **2010**, *18*, 2768-2773. (f) Efthymiou, C. G.; Stamatatos, T. C.; Papatriantafyllopoulou, C.; Tasiopoulos, A. J.; Wernsdorfer, W.; Perlepes, S. P.; Christou, G. *Inorg. Chem.* **2010**, *49*, 9737-9739. (g) Pasatoiu, T. D.; Sutter, J.-P.; Madalan, A. M.; Fellah, F. Z. C.; Duhayon, C.; Andruh, M. *Inorg. Chem.* **2011**, *50*, 5890-5898. (h) Cimpoesu, F.; Dahan, F.; Ladeira, S.; Ferbinteanu, M.; Costes, J.-P. *Inorg. Chem.* **2012**, *51*, 11279-11293. (i) Ke, H.; Zhao, L.; Guo, Y.; Tang, J. *Inorg. Chem.* **2012**, *51*, 2699-2705. (j) Abtab, S.M.T.; Maity, M.; Bhattacharya, K.; Sañudo, E. C.; Chaudhury, M. *Inorg. Chem.* **2012**, *51*, 10211-10221. (k) Xiong, K.; Wang, X.; Jiang, F.; Gai, Y.; Xu, W.; Su, K.; Li, X.; Yuana, D.; Hong, M. *Chem. Commun.* **2012**, *48*, 7456-7458. (l) Towatari, M.; Nishi, K.; Fujinami, T.; Matsumoto, N.; Sunatsuki, Y.; Kojima, M.; Mochida, N.; Ishida, T.; Re, N.; Mrozinski, J. *Inorg. Chem.* **2013**, *52*, 6160-6178. (m) Bhunia, A.; Yadav, M.; Lan, Y.; Powell, A. K.; Menges, F.; Riehn, C.; Niedner-Schatteburg, G.; Jana, P. P.; Riedel, R.; Harms, K.; Dehnend, S.; Roesky, P. W. *Dalton Trans.* **2013**, *42*, 2445-2450. (n) Chakraborty, A.; Bag, P.; Rivière, E.; Mallah, T.; Chandrasekhar, V. *Dalton Trans.* **2014**, *43*, 8921-8932. (o) Pasatoiu, T. D.; Etienne, M.; Madalan, A. M.; Andruh, M.; Sessoli, R. *Dalton Trans.* **2010**, *39*, 4802-4808. (p) Colacio, E.; Ruiz-Sanchez, J.; White, F. J.; Brechin, E. K., *Inorg. Chem.* **2011**, *50*,

7268-7273. (q) Mondal, K. C.; Kostakis, G. E.; Lan, Y.; Wernsdorfer, W.; Anson, C. E.; Powell, A. K. *Inorg. Chem.* **2011**, *50*, 11604-11611. (r) Okazawa, A.; Nojiri, H.; Ishida, T.; Kojima, N. *Polyhedron* **2011**, *30*, 3140-3144. (s) Sakamoto, S.; Fujinami, T.; Nishi, K.; Matsumoto, N.; Mochida, N.; Ishida, T.; Sunatsuki, Y.; Re, N. *Inorg. Chem.* **2013**, *52*, 7218-7229. (t) Zhao, L.; Wu, J.; Ke, H.; Tang, J. *Inorg. Chem.* **2014**, *53*, 3519-3525.

(11) (a) Hosoi, A.; Yukawa, Y.; Igarashi, S.; Teat, S. J.; Roubreau, O.; Evangelisti, M.; Cremades, E.; Ruiz, E.; Barrios, L.A.; Aromí, G.; *Chem. Eur. J.* **2011**, *17*, 8264-8268. (b) Peng, J. B.; Zhang, Q. C.; Kong, X. J.; Ren, Y. P.; Long, L. S.; Huang, R. B.; Zheng, L. S.; Zheng, Z. *Angew. Chem., Int. Ed.* **2011**, *50*, 10649-10652. (c) Peng, J. B.; Zhang, Q. C.; Kong, X. J.; Zheng, Y. Z.; Ren, Y. P.; Long, L. S.; Huang, R. B.; Zheng, L. S. *J. Am. Chem. Soc.* **2012**, *134*, 3314-3317. (d) Wang, P.; Shannigrahi, S.; Yakovlev, N. L.; Hor, T. S. A. *Chem. Asian J.*, **2013**, *8*, 2943. (e) Li, Z. Y.; Zhu, J.; Wang, X. Q.; Ni, J.; Zhang, J. J.; Liu, S. Q.; Duan, C. Y.; *Dalton Trans.* **2013**, *42*, 5711-5717. (f) Pineda, E. M.; Tuna, F.; Zheng, Y.-Z.; Winpenny, R. E.; McInnes, E. J. *Inorg. Chem.* **2013**, *52*, 13702-13707. (g) Wang, P.; Shannigrahi, S.; Yakovlev, N. L.; Hor, T. S. *Dalton Trans.* **2014**, *43*, 182-187. (h) Das, S.; Dey, A.; Kundu, S.; Biswas, S.; Mota, A. J.; Colacio, E.; Chandrasekhar V. *Chem. Asian J.*, **2014**, *9*, 1876. (i) Upadhyay, A.; Komatireddy, N.; Ghirri, A.; Tuna, F.; Langley, S. K.; Srivastava, A. K.; Sañudo, E. C.; Mobaraki, B.; Murray, K. S.; McInnes, E. J.; Affronte, M.; Shanmugam, M. *Dalton Trans.* **2014**, *43*, 259-266.

(12) (a) Pardo, E.; Ruiz-García, R.; Cano, J.; Ottenwaelder, X.; Lescouëzec, R.; Journaux, Y.; Lloret, F.; Julve, M. *Dalton Trans.* **2008**, *21*, 2780. (b) Palacios, M. A.; Rodríguez-Diéguez, A.; Sironi, A.; Herrera, J. M.; Mota, A. J.; Cano, J.; Colacio, E. *Dalton Trans.* **2009**, *40*, 8538. (c) Colacio, E.; Palacios, M. A.; Rodríguez-Diéguez, A.;

- Mota, A. J.; Herrera, J. M.; Choquesillo-Lazarte, D.; Clérac, R. *Inorg. Chem.* **2010**, *49*, 1826.
- (13) Zeyrek, C. T.; Elmali, A.; Elerman, Y.; Svoboda, I. *Z. Naturforsch.* **2005**, *60b*, 143.
- (14) APEX2, Bruker AXS, Madison, WI, 2010.
- (15) SAINT, version 8.30a, Bruker AXS, Madison, WI, 2013.
- (16) Sheldrick, G. M. SADABS, version 2004/1, Bruker AXS, Madison, WI, 2008.
- (17) Sheldrick, G. M. *Acta Crystallogr A* **2008**, *64*, 112.
- (18) Dolomanov, O. V.; Bourhis, J.; Gildea, R. J.; Howard, J. A. K.; Puschmann, H., *J. Appl. Cryst.* **2009**, *42*, 339.
- (19) (a) Clarke, B.; Clarke, N.; Cunningham, D.; Higgins, T.; McArdle, P.; Cholchúin, M. N.; O’Gara, M. *J. Organomet. Chem.* **1998**, *559*, 55.
- (20) Llunell, M.; Casanova, D.; Cirera, J.; Bofill, J. M.; Alemany, P.; Alvarez, S.; Pinsky, M.; Avnir, D. SHAPE v1.1b, Barcelona, **2005**.
- (21) (a) Yamaguchi, T.; Sunatsuki, Y.; Kojima, M.; Akashi, H.; Tsuchimoto, M.; Re, N.; Osa, S.; Matsumoto, N., *Chem. Commun.* **2004**, 1048–1049. b) Igarashi, S.; Kawaguchi, S.; Yukawa, Y.; Tuna, F.; Winpenny, R. E. P. *Dalton Trans.* **2009**, *17*, 3140. (b), Cristóvão B.; Pelka R., Mirosław B.; Klak J., *Inorg. Chem. Commun.* **2014**, *46*, 94.
- (22) (a) Feltham, H. L. C.; Lan, Y.; Klöwer, F.; Ungur, L.; Chibotaru, L. F.; Powell, A. K.; Brooker, S. *Chem. Eur. J.* **2011**, *17*, 4362. (b) Bi, Y.; Guo, Y.-N.; Zhao, L.; Guo, Y.; Lin, S.-Y.; Jiang, S. D.; Tang, J.; Wang, B. W.; Gao, S. *Chem. Eur. J.* **2011**, *17*, 12 476 and references. (c) Ruiz, J.; Mota, A. J.; Rodríguez-Diéguez, A.; Titos, S.; Herrera, J. M.; Ruiz, E.; Cremades, E.; Costes, J. P.; Colacio, E. *Chem. Commun.* **2012**, *48*, 7916.
- (23) Bhunia, A.; Gamer, M. T.; Ungur, L.; Chibotaru, L. F.; Powell, A. K.; Lan, Y.; Roesky, P. W.; Menges, F.; Riehn, C.; Niedner-Schatteburg, G. *Inorg. Chem.* **2012**, *51*, 9589.

- (24) Chandrasekhar, V.; Bag, P.; Kroener, W.; Gieb, K.; Müller, P. *Inorg. Chem.* **2013**, *52*, 13078.
- (25) Rinehart, J. D.; Fang, M.; Evans, W. I.; Long, J. R., *Nature Chemistry*, **2011**, *3*, 538-542.
- (26) Ungur, L.; Thewissen, M.; Costes, J.-P.; Wernsdorfer, W.; Chibotaru, L. F. *Inorg. Chem.* **2013**, *52*, 6328.
- (27) Boca, R. *Coord. Chem. Rev.* **2004**, *248*, 757.
- (28) Singh, K.; Tibrewal, N. K.; Rajaraman, G. *Dalton Trans.* **2011**, *40*, 10897 and references therein.
- (29) Paital, A. R.; Mitra, T.; Ray, D.; Wong, W. T.; Ribas-Ariniño, J.; Novoa, J. J.; Ribas, J.; Aromi, G. *Chem. Commun.*, **2005**, *41*, 5172.
- (30) (a) Hou, Y.-L.; Xiong, G.; Shi, P.-F.; Cheng, R. R.; Cui, J.-Z.; Zhao, B.; *Chem. Commun.* **2013**, *49*, 6066. (b) Lorusso, G.; Sharples, J. W.; Palacios, E.; Roubeau, O.; Brechin, E. K.; Sessoli, R.; Rossin, A.; Tuna, F.; McInnes, E. J. L.; Collison, D.; Evangelisti, M. *Adv. Mater.* **2013**, *25*, 4653. (c) Sibille, R.; Mazet, T.; Malaman, B.; François, M.; *Chem. Eur. J.* **2012**, *18*, 12970.
- (31) Guo, F.-S.; Chen, Y.-C.; Liu, J.-L.; Leng, J.-D.; Meng, Z. S.; Vrábel, P.; Orendáč, M.; Tong, M.-L. *Chem. Commun.* **2012**, *48*, 12219.